Development 122, 1811-1819 (1996)
Printed in Great Britain © The Company of Biologists Limited 1996
DEV0065

LOP1: a gene involved in auxin transport and vascular patterning in *Arabidopsis*

Francine M. Carland[1] and Neil A. McHale*

Department of Biochemistry and Genetics, The Connecticut Agricultural Experiment Station, P.O. Box 1106, New Haven, CT 06504, USA

[1]Present address: Department of Biology, Yale University, New Haven, CT 06520-8104, USA
*Author for correspondence

SUMMARY

We have taken a genetic approach to understanding the mechanisms that control vascular patterning in the leaves of higher plants. Here we present the identification and characterization of the *lop1* mutant of *Arabidopsis* which is defective in basipetal transport of IAA. Mutant leaf midveins show disoriented axial growth, and bifurcation into twin veins that are frequently rotated out of the normal dorsal/ventral axis of the leaf. Mutant plants also display abnormal patterns of cell expansion in the midrib cortex and in the epidermis of the elongation zone of lateral roots. Lateral roots show abnormal curvature during initiation, sometimes encircling the primary root prior to growth in a normal downward direction. Mutant seedlings have normal levels of free IAA, and appear normal in auxin perception, suggesting that transport is the primary lesion. The abnormalities in vascular development, lateral root initiation and patterns of cell expansion observed in the *lop1* mutant are consistent with a basic disruption in basipetal transport of IAA.

Key words: auxin transport, *Arabidopsis* mutant, vascular patterning, *lopped*, IAA

INTRODUCTION

The role of translocatable signal molecules in plant development was first proposed by Darwin in the nineteenth century as an explanation for phototropism (Lomax et al., 1995). It was later demonstrated that this capacity for directional growth in higher plants was indeed governed by lateral redistribution of indole-3-acetic acid (IAA), a naturally occurring plant hormone in the auxin family. Auxin has since been shown to influence other aspects of plant development, most notably the differentiation of vascular tissue. A large body of evidence shows that auxin synthesized by leaf primordia is an inductive signal for vascular differentiation in the shoot (Shininger, 1979). Surgical manipulation of the shoot apex revealed that leaf primordia are essential for basipetal development of primary xylem (Young, 1954; Wangermann, 1967). The inductive effect of the leaf can be replaced by application of auxin or with auxin and sucrose (Young, 1954; Jacobs and Morrow, 1957). Similarly, shoot tips grafted to undifferentiated callus induce xylem formation, and the response is mimicked by application of auxin (Wetmore and Rier, 1963). Auxin appears to play a similar role in differentiation of the primary phloem (LaMotte and Jacobs, 1963). Manipulation of IAA levels in transgenic plants also supports a primary role for this hormone in vascular differentiation. Transgenic petunia plants with ten-fold overproduction of IAA show an increase in production of secondary xylem and phloem (Klee et al., 1987), and conversely, auxin inactivation in transgenic tobacco produces an inhibition of vascular differentiation (Romano et al., 1991).

Although it is clear that auxin plays an essential role in formation of vascular tissue, the mechanisms for spatial regulation of this process and ultimate elaboration of reproducible venation patterns in the leaf remain largely unexplored. Our current insights have arisen mostly from experiments involving redifferentiation of xylem elements in plant stems following application of IAA (Sachs, 1991). This work demonstrates that experimental redirection of auxin flow around wound sites produces a reorientation in the polarity of cell elongation and a correlated change in the path of vascular differentiation. This is thought to begin with formation of specialized, elongated cell files for basipetal auxin transport in a process known as 'canalization'. According to the canalization hypothesis (Sachs, 1991), formation of a specialized path for auxin flow leads directly to axial elongation of transporting cells and their subsequent differentiation into vascular elements. The molecular basis for basipetal auxin transport is thought to involve establishment of an intracellular asymmetry for membrane-localized protein carriers with specific roles in IAA uptake and efflux (Lomax et al., 1995). Localization of IAA efflux carriers at the basipetal end of the cell is considered to be the primary mechanism establishing the polarity of auxin transport.

Identification of genes involved in the positioning of these specialized channels for auxin transport will be an important step toward understanding the molecular basis of vascular patterning. Mutations at the *PIN-FORMED* locus on chromosome 1 in *Arabidopsis* produce a disruption in IAA transport (14% of wild-type) and a deficiency in levels of free IAA (8% of wild-type) (Okada et al., 1991). Mutant *pin1* plants have an

abnormal spike inflorescence lacking floral buds and fused cotyledons, suggesting that this genes plays a role in flower initiation and during embryogenesis. Mutant leaves also show split midveins, supporting a role for this gene in leaf vascular patterning. In the absence of any other mutations in the transport pathway, however, our knowledge of the process remains quite rudimentary.

We have initiated a mutational analysis in *Arabidopsis* aimed at understanding the molecular basis for vascular patterning in dicot leaves. Here we report the recovery and characterization of a recessive mutation (*lop1*) that produces a major defect in basipetal transport of IAA. Mutant midveins show disoriented axial growth, and bifurcation into twin veins that are frequently rotated out of the normal dorsal/ventral axis of the leaf. In addition mutants show abnormal patterns of cell expansion in the midrib cortex and in the root epidermis that are consistent with a disruption in IAA transport.

MATERIALS AND METHODS

Plant material and growth conditions

The T-DNA collection, the ecotype Landsberg *erecta*, and the *axr1-3* and *axr1-12* mutants were obtained from the Arabidopsis Biological Resource Center (ABRC, Ohio State). Plants were grown in Metro Mix 200 (Grace) at 22°C and 60-70% relative humidity with 16 hours illumination. For plating seed on media, the seeds were surface sterilized by immersion in 20% hypochlorite/0.05% Tween followed by several rinses with sterile water. The seeds were allowed to air dry and then plated on an MSG medium (Murashige and Skoog, 1962) at 0.5× major salts, 1% sucrose, and no hormones. Plants were grown at 27°C under continuous illumination. The T-DNA collection was screened from plants grown in Metro Mix as described above.

Genetic and linkage analysis

A homozygous *lop1* plant (ecotype Ws) was used as the pistillate parent in a cross with wild-type Landsberg *erecta*. Seed was collected from individual F_1 plants yielding a polymorphic F_2 population. *Arabidopsis* genomic DNA was isolated from individual F_2 plants grown in soil or from pools of >20 individuals in an F_3 family grown on MS plates. All wild-type F_2 plants (*LOP1*/*LOP1* and *LOP1*/*lop1*) were progeny tested providing an informative population for mapping purposes. Because *lop1* is male sterile, the F_3 pools consisted of plants either homozygous or heterozygous for the wild-type allele.

For PCR analysis, DNA was isolated using the method of Dellaporta et al. (1994). Amplification was performed in a Perkin Elmer thermal cycler as described by Bell and Ecker (1994) although more consistent reactions were obtained when approximately 25 ng of DNA was used in the reaction. For nga76, the annealing temperature was lowered from 55°C to 50°C. PCR products were resolved by electrophoresis on either 2% ultrapure agarose (Gibco BRL)/2% Nusieve, 1× TAE or 3-4% Metaphor (FMC, Rockland, ME) in 1× TBE (89 mM Tris borate, 2 mM EDTA) depending on the size of the different alleles. Microsatellite primers were obtained from Research Genetics (Huntsville, AL). For Southern blot analysis, plant DNA was isolated as above except extractions with phenol followed by phenol/choloroform/isoamyl alcohol (50:48:2) were included prior to precipitation of DNA with isopropanol. Standard methods were used for plasmid and cosmid DNA preparations, Southern blots and hybridizations with probes labeled by random priming (Sambrook et al., 1989). Chromosome five RFLP markers were obtained from the ABRC (Ohio State). The cosmid RFLP marker 558A had been subcloned and converted to an ARMS marker (Fabri and Schaffner, 1994) providing a marker in plasmid form. For initial mapping studies using the microsatellite primers, a population consisting of 29 plants (58 chromosomes) was analyzed. For further localization of *lop1* using additional chromosome 5 markers, a population consisting of 46 plants (92 chromosomes) was examined.

Multipoint linkage analysis was performed using a Macintosh version of MAPMAKER (version VI, Lander et al., 1987). Recombination frequencies from multipoint analysis were converted into map distances (centiMorgans) using the Kosambi function (Kosambi, 1944) and integrated with the existing molecular genetic map (Hauge et al. 1993).

axr1,lop1 double mutants

Mutant strains homozygous for the *axr1-3 a*nd *axr1-12* mutations were employed in a double mutant analysis. Under our growth conditions, both *axr1* mutants had similar phenotypes. Both mutants were hybridized with *LOP1/lop1* heterozygotes. The analysis of *lop1, axr1-3* and *lop1, axr1-12* F_2 progenies was conducted separately, but gave similar results and the data were subsequently pooled. Double heterozygotes were identified as F_1 individuals segregating the *axr1* and *lop1* mutations, along with a rare novel phenotype. The frequency of F_2 phenotypic classes was scored in MSG plates and subjected to χ^2 analysis.

Histology

Plant materials were prepared for sectioning by overnight fixation in ethanol-chloroform-glacial acetic acid (6:3:1 v/v), followed by stepwise infiltration first with butanol and then with melted paraffin at 60°C in a vacuum oven. Sections (8 μm) were cut from paraffin blocks, fixed to glass slides and dried overnight prior to staining with hemalum and safranin as previously described (McHale, 1993). Wild-type and mutant leaves were cleared by fixation in 70% ethanol and dehydration in 100% ethanol, followed by overnight incubation in saturated chloral hydrate.

Scanning electron microscopy

Samples were prepared for scanning electron microscopy by overnight fixation in ethanol-chloroform-glacial acetic acid (6:3:1) that was followed by stepwise transfer to 100% ethanol, and critical point drying with liquid carbon dioxide in a Polaron pressure chamber. Dried samples were mounted on stubs, sputter coated, and examined with an ISI-SS40 scanning electron microscope.

Auxin assays

To compare levels of free IAA in mutant and wild-type plants, we grew an F_3 family segregating the *lop1* mutation on MS medium with 2% sucrose in Petri plates, and harvested the aerial portion of mutants and normals at 11 days postgermination. Triplicate samples were frozen in liquid N_2 and ground in a mortar (65% isopropanol in 0.2 M imidazole, pH 7.0). Samples were spiked with 100 ng [$^{13}C_6$]IAA and [^{3}H]IAA (26 Ci/mmol), diluted to 10% isopropanol, applied to amino ion exchange columns (PrepSep 0.3g Fisher), washed (sequentially with 2 ml hexane, ethylacetate, acetonitrile, methanol), eluted with 3 ml methanol/2% acetic acid, dried and resuspended in 100 μl 50% methanol for HPLC (Phenomenex, UltraCarb 30), using 20% methanol in H_2O/1% acetic acid for elution. Samples were assayed by mass spectrometry by Dr Jennifer Normanly (Department of Biochemistry and Molecular Biology, University of Massachusetts) by the method of Chen et al. (1988).

Auxin response was assayed by measuring root growth of mutant and wild-type seedlings in the presence of exogenous 2,4D at 0.5, 1, 3 and 6×10^{-8} M. An F_3 family segregating the *lop1* mutation was grown for 6 days on an MS medium with 2% sucrose. Mutant and wild-type siblings were transferred separately to media containing 2,4D, and to MS control plates with no 2,4D. The root system was positioned on the agar surface to allow measurement of new growth (downward) at daily intervals up to 12 days postgermination.

Auxin transport was assayed in excised inflorescence stems of soil-grown mutant and wild-type siblings as described by Okada et al.

(1991). The [^{14}C]IAA was purchased from the Sigma Chemical Company, St. Louis, MO.

RESULTS

Isolation and mapping

Our strategy for the genetic analysis was to isolate putative vascular mutants generated by T-DNA insertion. We screened 100,000 plants in pools of T4 seed (Feldmann collection: CS 2606-2654 from ABRC) representing 5,000 independent T-DNA insertion events, and self-pollinated or outcrossed the aberrant leaf variants for further analysis. One variant with normal cotyledons and narrow, deformed leaves was male-sterile, but outcrossed as pistillate parent to wild-type Landsberg *erecta*. Pooled data from three independent F_2 families showed segregation ratios conforming to the 3:1 pattern (272 normal: 90 mutant) expected for a single recessive mutation. Because mutant leaves displayed sporadic occurrence of bladeless regions along the midrib, the mutation was named *lopped* and the mutant allele designated *lop1*. Southern blot analysis using various T-DNA probes revealed that *lop1* did not contain a T-DNA insert. Microsatellite primers were used to position *lop1* on the molecular genetic map. *lop1* was found to be linked to marker nga129 at the bottom of chromosome five, as shown in Fig. 1. Additional RFLP molecular markers (g4130, m558, and g3844) further localized *lop1* to the position 83.0±2.0, as described in Materials and Methods.

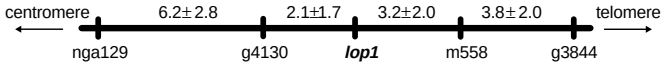

Fig. 1. Map position for the *LOP1* gene on chromosome 5 of *Arabidopsis*. Numbers above the horizontal line represent map distances in centimorgans ± standard error between adjacent markers.

Table 1. Developmental leaf morphology in *Arabidopsis*

Stage	Length (mm)	Morphology
1	0.05-0.1	Curved over apex
2	0.1-0.2	Upright, trichome initiation
3	0.2-0.5	Tip trichomes, 1° lobes visible, ventral midrib visible
4	0.5-1.0	Tip curvature, tip to base trichomes, 2° and 3° lobes visible, petiole visible
5	1.0	Petiole elongation

Wild-type leaf development

To facilitate the comparison of mutant leaf phenotypes to wild-type, stages in the development of wild-type rosette leaves of *Arabidopsis* were assigned based on leaf length and appearance of distinct morphological landmarks, as described in Table 1 and shown in Fig. 2A-E.

At stage 1, leaf primordia are 0.05-0.1 mm in length and curved over the shoot apical meristem (Fig. 2A). At stage 2, primordia are 0.1-0.2 mm long and show an upright stature, and trichomes are initiated on the dorsal surface toward the tip of the blade (Fig. 2A). At stage 3 (0.2-0.5 mm), developed trichomes are visible at the leaf tip, and primary lobes of the blade are initiated (Fig. 2B). The midrib also becomes visible at this stage through expansion of ventral epidermal cells subtending the developing midvein, and elongated epidermal cells appear at the margin of the leaf blade. At stage 4 (0.5-1.0 mm), the tip of the leaf curves away from the shoot axis, and trichomes are observed from the tip to the base of the blade. Petiole elongation begins, and secondary and tertiary lobes (below the primary lobes) are initiated at the blade/petiole junction (Fig. 2C). During stage 5 (>1 mm, Fig. 2D,E) petiole elongation continues, and files of expanded ventral epidermis associated with the

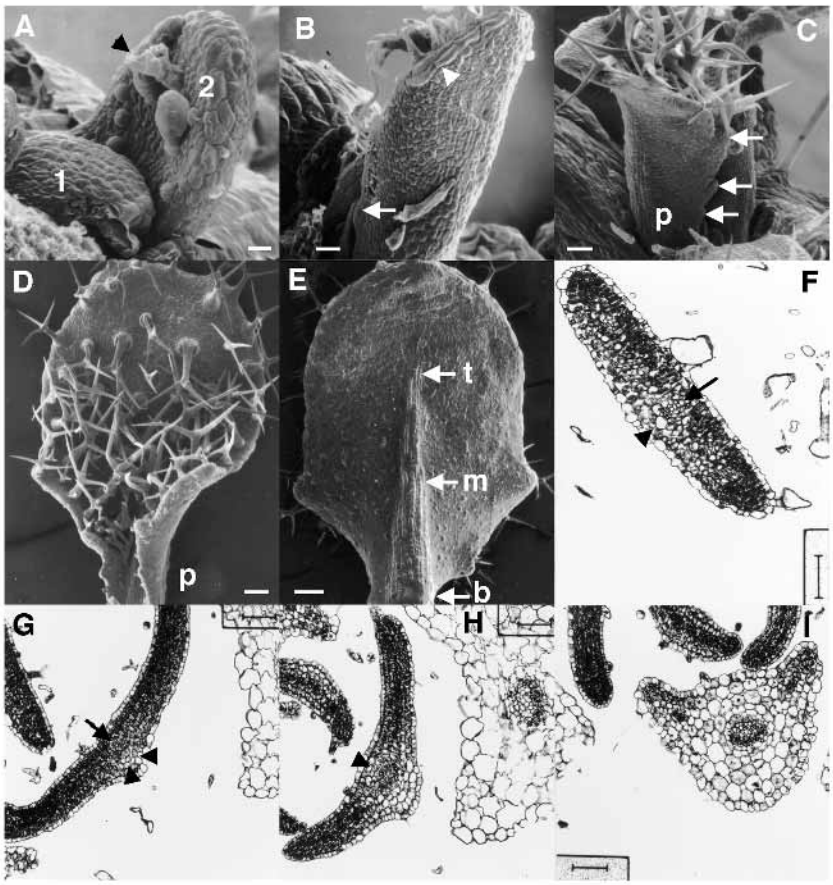

Fig. 2. Developmental morphology and anatomy in wild-type leaves of *Arabidopsis*. Scanning electron micrographs show morphological landmarks for developing leaves. (A) Stages 1 and 2; arrow shows trichome initiation; bar, 10 μm. (B) Stage 3; arrow shows lobe initiation; arrowhead shows elongated epidermal cells at the blade margin; bar = 20 μm. (C) Stage 4; p, petiole; arrows (top to bottom) show 1°, 2° and 3° lobes; bar, 40 μm. (D) Dorsal leaf surface at stage 5; p, petiole; bar, 100 μm. (E) Ventral leaf surface at stage 5; t,m,b, tip, middle and base of the midrib, respectively; bar, 100 μm. Transverse sections (20×) through the tip, middle and base of stage 4 leaves show developmental stages in formation of the midrib; bars, 50 μm. (F) Tip; arrow shows the midvein; arrowhead shows vein-proximal cell expansion in the ventral mesophyll. (G) Middle; arrow shows the midvein; arrowheads show formation of ventral rib cortex. (H) Middle; arrowhead shows vein-proximal cell expansion in the dorsal mesophyll. (I) Base of leaf.

midrib extend from the leaf base upward through approximately 75% of the total leaf length.

Wild-type midrib anatomy

Anatomical analysis of leaf midrib development was carried out by examination of serial transverse sections along the rib axis from tip to base in stage 4 leaves, as shown in Fig. 2F-I. Sections through the tip of the midvein show that the earliest evidence of rib development is vacuolation and expansion of ventral mesophyll cells subtending the vein (Fig. 2F). The upper mesophyll is unaffected at this stage, and there is no evidence of epidermal cell expansion. Protrusion of the midrib is first observed on the lower surface of the leaf (Fig. 2G). This process involves localized division and expansion of vein-proximal cells in the ventral cortical region, along with expansion of the subtending epidermis (Fig. 2E,G). The next stage in rib development is marked by a similar pattern of cortical development on the dorsal side of the vein (Fig. 2H). Vein proximal cells of the upper mesophyll show vacuolation and expansion, periclinal cell divisions have generated an additional layer of cortical cells, and epidermal cell expansion is visible. Sections through the region at the blade/petiole junction show that this developmental pattern persists in the later stages of rib development (Fig. 2I). The ventral cortical region shows 4-5 layers of vacuolated cells that account for protrusion of the rib on the underside of the leaf. Formation of 2-3 layers of dorsal cortex generates a visible rib on the upper surface as well. At this stage, vacuolated cortical cells are also observed on the lateral flanks of the midvein, generating a radial pattern of rib growth. Cell size increases with increasing distance from the vein in all directions, suggesting that addition of cortical layers involves division of the vein proximal cells.

lop1 mutant phenotype

Morphological and anatomical aberrations associated with the *lop1* mutation are shown in Fig. 3. Mutant plants germinate normally and have normal cotyledons, but all of the true leaves are deformed and dwarfed (Fig. 3B) relative to wild-type (Fig. 3A). The placement and timing of leaf initiation is normal in the mutant, suggesting that the basic programs of the shoot meristem are not affected by the mutation. Mutant plants show a variety of morphological aberrations including twisting of the leaf petiole (Fig. 3E) and the style of the flowers (Fig. 3C). In extreme cases, twisting of the leaf petiole results in a 180° rotation of the leaf away from the shoot axis. Mutant leaves show disruptions in development of the midvein, including general disorientation in the direction of growth (Fig. 3D), and bifurcation into twin veins that fail to initiate the normal series of lateral branches (Fig. 3G). This is in contrast to wild-type leaves which show the typical netted venation of dicots, with a fixed set of main lateral branches joining a single central midvein (Fig. 3F). The *lop1* mutation also produces abnormal development of the root system. In wild-type plants, lateral roots are initiated at right angles to the primary root, as shown in Fig. 3I. In contrast, lateral roots of the mutant show random patterns of curvature during initiation (Fig. 3J), and sometimes encircle the primary root before establishing growth in a normal downward direction.

lop1 leaf morphology and anatomy

The developmental morphology and anatomy of *lop1* mutant leaves are shown in Fig. 4.

Stage 1 primordia have a normal morphology, but stage 2 primordia show emergence of marginal protrusions (Fig. 4A) that develop as independent growing points in the expanding blade (Fig. 4C). These protrusions typically emerge in the position for the primary lobes of the leaf, although well ahead of the stage when they normally appear in wild-type (stage 3, Fig. 2B). Newly initiated protrusions can be observed in the blade of stage 4 leaves, indicating that this process extends over

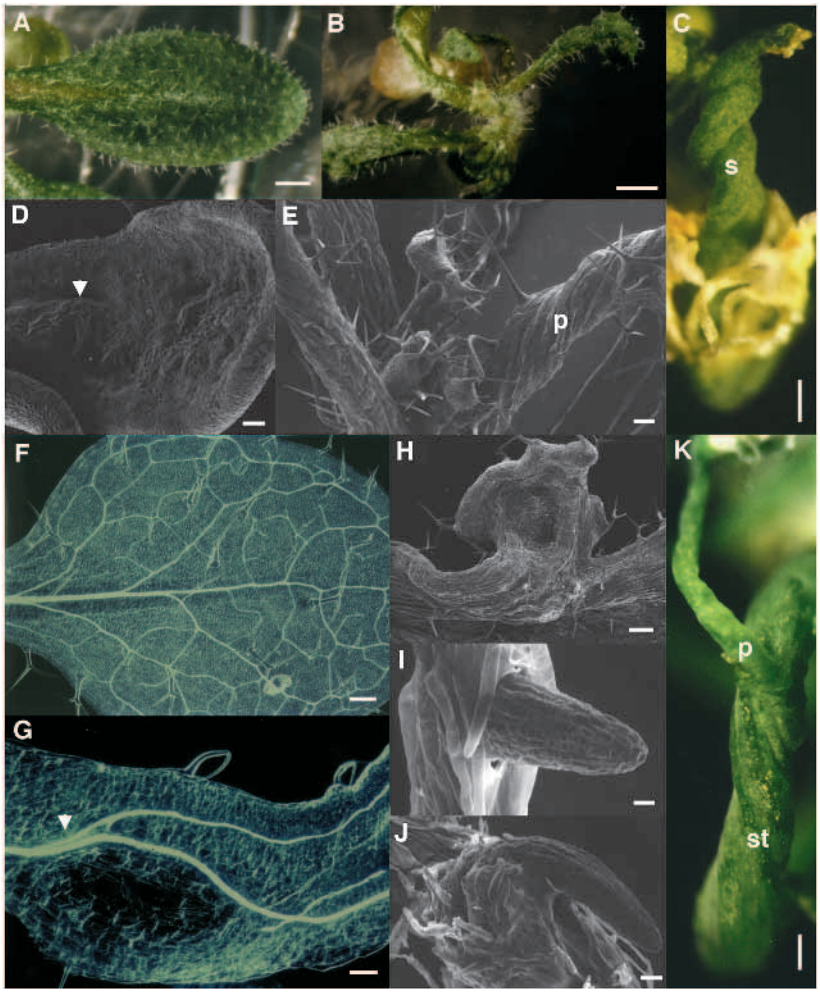

Fig. 3. Phenotypic effects of the *lop1* mutation in *Arabidopsis*. (A) Wild-type leaf; bar, 2 mm. (B) *lop1* seedling; bar, 2 mm. (C) *lop1* flower with twisted carpel. s, style, bar, 500 μm. (D) *lop1* ventral leaf surface; arrowhead shows disoriented midrib; bar, 100 μm. (E) *lop1* seedling. p, twisted petiole; bar, 100 μm. (F) Cleared wild-type leaf showing normal venation; bar, 100 μm. (G) Cleared *lop1* leaf; arrowhead shows midvein bifurcation; bar, 100 μm. (H) Vascularized protrusion on margin of *lop1* leaf; bar, 100 μm. (I) Wild-type lateral root; bar, 20 μm. (J) *lop1* lateral root showing abnormal curvature; bar, 20 μm. (K) *lop1* twisted inflorescence stem; p, pedicel; st, stem; bar, 500 μm.

several stages of leaf development (Fig. 4D). Early stages of midrib development appear normal in stage 3 leaves (Fig. 4B), but disorientation of midrib growth is evident by stage 4 (Fig. 4C). In mutant leaves at stage 5, there are two abnormal midrib phenotypes that are associated with abnormal vascular patterning. The midrib can develop as a centrally located oversized structure (Fig. 4E), or it can show bifurcation and develop as two distinct ribs located at the leaf margins (Fig. 4G). Transverse sections through the blade/petiole junction of these leaves is shown in Fig. 4F and H, respectively. In both cases, twin vascular regions are observed indicating a bifurcation of the developing midvein. The twins are usually disoriented and in some cases are rotated 90° relative to one another (Fig. 4F). In contrast, vascular tissue in a wild-type midvein shows a uniform alignment along a single dorsal/ventral axis in the leaf, with the xylem and phloem poles facing the dorsal and ventral surfaces, respectively (Fig. 2I).

The transverse section in Fig. 4I shows stage 2 and stage 3 wild-type leaves. The stage 2 leaf shows meristematic divisions throughout the mesophyll, and no evidence of cortical cell expansion. At stage 3, radial expansion is visible in the ventral cortical cells subtending the midvein. In contrast, the mutant stage 2 leaf in Fig. 4J shows precocious expansion of cortical cells on the ventral surface of the primordium. Similarly, the mutant stage 3 leaf shows a broad zone of precocious cortical expansion on the ventral side of the midrib. Median transverse sections through mutant leaves at stage 4 (Fig. 4K) frequently show a one-sided blade morphology that is associated with precocious expansion of cortical cells along the lateral flank (compare to median wild-type sections, Fig. 2G,H).

To quantitate patterns of cortical cell expansion in the midrib, cellular dimensions were measured in mutant leaves and matched wild-type controls, as shown in Table 2. Cortical cell number and size and overall rib dimensions were examined at progressive stages of rib formation (tip to base) in stage 4 and stage 5 leaves. The data show that development of the wild-type midrib cortex involves both cell division and cell expansion. In stage 5 leaves, there is a doubling of cortical cell layers (ventral) and a 2.5-fold increase in cortical cell size at the midrib base relative to the tip. Data from mutant leaves (stage 4 and 5) show that the tip of the midrib is significantly larger than the wild-type control both in the dorsal/ventral and the lateral axis. Cortical cell data show that cell number is unchanged relative to wild-type, and that the increase in rib size reflects an increase in cell size. The transect diameter of the largest cortical cell in the mutant leaves (20 μm) is double that of wild-type. A similar pattern is observed at the base of the midrib. Mutant ribs are larger than wild-type, again reflecting primarily an increase

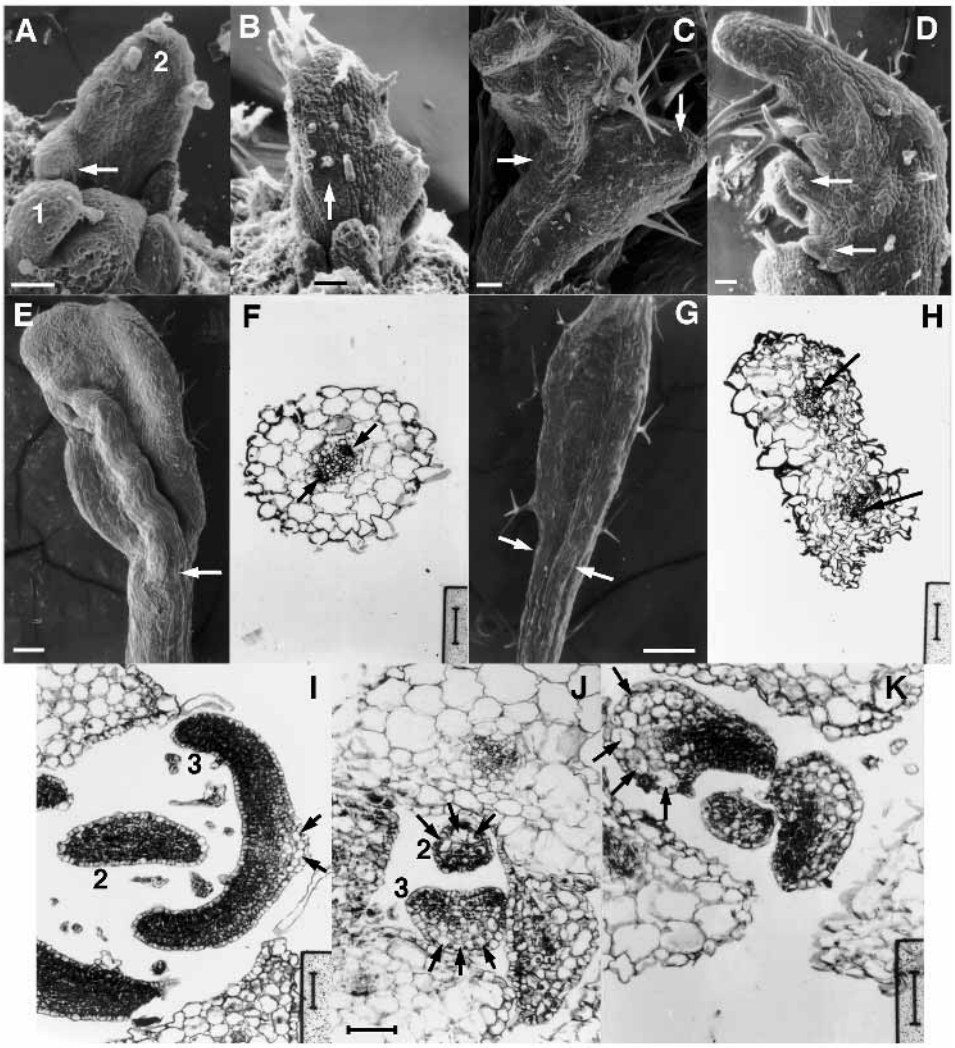

Fig. 4. Leaf development and vascular patterning in *lop1* mutant leaves. (A) Normal morphology in stage 1, and marginal protrusions (arrow) in stage 2 primordia; bar, 25 μm. (B) Normal midrib formation (arrow) on ventral surface of a stage 3 primordium; bar, 25 μm. (C) Midrib disorientation in a stage 4 leaf (horizontal arrow), and formation of independent growing points (vertical arrow) in the blade; bar, 25 μm. (D) Initiation of marginal protrusions (arrows) in a stage 4 leaf; bar, 25 μm. (E) Oversized central midrib in a stage 5 leaf; arrow marks the position of the transverse section shown in F; bar, 100 μm. (F) Transverse section showing the anatomy in the petiole of a stage 5 leaf (E), with twin midveins in mirror image orientation; arrows show misaligned phloem poles; bar, 50 μm. (G) Twin ribs along the margins of a stage 5 leaf; arrows mark the position of the transverse section shown in H; bar, 50 μm. (H) Disoriented twin veins at the blade/petiole junction in a stage 5 leaf (G); arrows show misaligned phloem poles; bar, 50 μm. (I) Wild-type shoot apex showing meristematic blade mesophyll (stage 2) and expansion of cortical cells (arrows) subtending the midrib (stage 3); bar, 50 μm. (J) Mutant shoot apex showing precocious radial expansion of cortical cells (arrows) in stage 2 and 3 primordia; bar, 50 μm. (K) Median transverse section of mutant stage 4 leaves showing precocious cortical expansion (arrows) associated with one-sided loss of blade formation; bar, 50 μm.

Table 2. Leaf midrib anatomy in wild-type and the *lop1* mutant of *Arabidopsis*

	Rib size (μm)		Cortex			Epidermis
	Dors/vent axis‡	Lateral axis§	Dorsal cell layers¶	Ventral cell layers**	Dorsal cell size (μm)††	Ventral cell number‡‡
Wild-type						
Stage 4						
Tip*	50	70	1	2	10	7
Base†	70	135	2	3	15	21
Stage 5						
Tip	80	80	1	2	10	5
Base	140	170	3	4	25	26
lop1						
Stage 4						
Tip	80	120	1	2	21	21
Base	100	135	2	3	25	25
Stage 5						
Tip	100	120	1	2	20	15
Base	145	200	3	4	35	25

Data represent the mean of measurements taken on four separate leaves.
*Midrib tip data were taken in the region where expansion of the rib epidermis becomes visible.
†Midrib base data were taken in the petiole below the lobed region of the blade.
‡Rib size in the dorsal/ventral axis.
§Rib size in the side/side axis.
¶Counts of cortical cell layers directly above the midvein.
**Counts of cortical cell layers directly below the midvein.
††Length of the longest axis in the largest ventral cortical cell.
‡‡Number of files of epidermal cells spanning the ventral side of the midrib.

in cortical cell size. The number of cortical cell layers on the dorsal and ventral sides of the midvein is unaffected.

The *lop1* mutation also produces abnormal patterns of cell expansion in epidermal cells of the root elongation zone, as shown in Fig. 5. In wild-type roots, expanding epidermal cells in the elongation zone remain aligned in distinct longitudinal files (Fig. 5A), whereas mutant roots show an irregular pattern of cell expansion in this region, and a deviation of cell files from their normal axial alignment into a spiralling pattern (Fig. 5B). This pattern persists in the elongation zone, ultimately generating lateral roots with a twisted morphology (Fig. 5D). During subsequent maturation, mutant roots become flattened and oblong in transverse view, and frequently show two parallel vascular systems (Fig. 5F). This appears to result from formation of new lateral roots that grow initially along the same axis as the primary root before emerging as a separate structures. In contrast, wild-type roots retain their cylindrical shape during maturation, and initiate new lateral roots at right angles to the primary axis (Fig. 5C,E).

Ethylene

Initially it seemed possible that the mutation was affecting the ethylene pathway, as this hormone can affect radial cell expansion (Abeles et al., 1992), and xylem differentiation (Aloni, 1987). Since ethylene overproducing mutants of *Arabidopsis* (*eto1*; Guzman and Ecker, 1990) show the well-known triple response phenotype (exaggerated apical hook, stunting, radial swelling), we examined hook and hypocotyl phenotypes in dark-grown *lop1* mutants and wild-type siblings, but found no observable difference (not shown). In addition, the ethylene inhibitors $AgNO_3$ and alpha amino isobutyric acid which abolish the triple response of *eto1* did not affect the *lop1* mutant phenotype. Thus it appeared from preliminary assays that the *lop1* phenotype was not the result of ethylene overproduction.

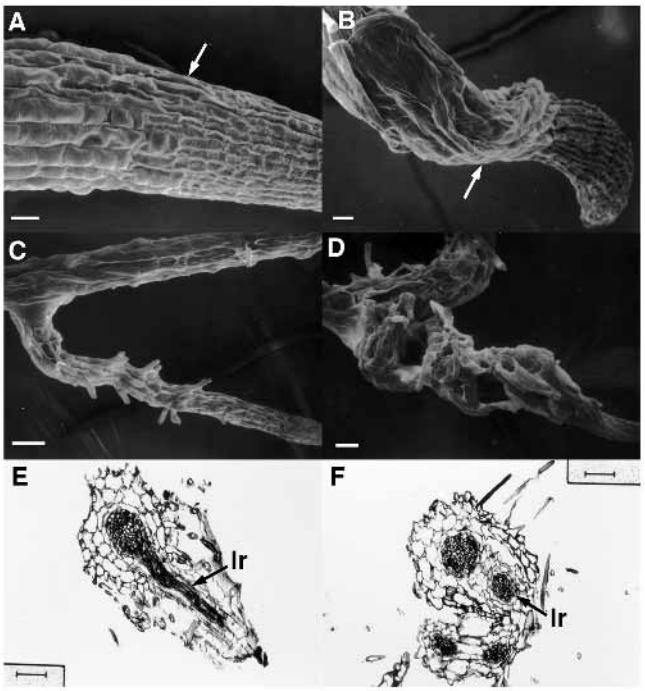

Fig. 5. Root morphology and anatomy in wild-type and the *lop1* mutant of *Arabidopsis*. (A) Wild-type root showing axial alignment of epidermal cell files in the elongation zone (arrow); bar, 10 μm. (B) Mutant root showing epidermal disorganization in the elongation zone (arrow); bar, 10 μm. (C) Wild-type lateral root; bar, 40 μm. (D) Mutant lateral root with twisted morphology; bar, 50 μm. (E) Transverse section through the vascular junction between a primary root and a lateral root (lr) in wild-type. The vascular system of the lateral root (arrow) shows a longitudinal orientation relative to a transverse vascular orientation in the primary root; bar, 62.5 μm. (F) Transverse section through a mutant primary root showing the vascular system of a lateral root (arrow) running parallel to the primary vascular system; bar, 62.5 μm.

Auxin levels

Our evidence for disruptions in vascular patterning and cell expansion in mutant plants raised the possibility that *lop1* affects a step in the auxin pathway. To determine whether the mutation affects endogenous levels of auxin, we assayed free IAA in mutant seedlings and wild-type controls at 11 days post-germination by GC-SIM-MS (Chen et al., 1988). Free IAA levels were virtually identical (1.25±0.09 ng IAA/mgfwt) in triplicate samples of mutant and wild-type seedlings. The majority of IAA in plants is conjugated to sugars, peptides, or amino acids by ester or amide linkages, and gradually released as free IAA, which is generally assumed to be the biologically active form (Normanly et al., 1995). Our results do not exclude the possibility that *lop1* is affecting the size or dynamics of these conjugated pools, but this would be expected to produce some alteration in levels of free IAA. A highly sensitive IAA assay produced no evidence for this, suggesting that *lop1* is not a biosynthesis mutant.

Table 3. Genotype frequency and root development in the F_2 progeny of *axr1,lop1* double heterozygotes

Genotype	F_2 frequency* Observed	F_2 frequency* Expected	Root length† (mm)
Wild-type	107	97	38.5±9.8
axr1	23	32	42.2±7.5
lop1	32	32	12.2±2.5
axr1, lop1	10	11	17.0±4.5

*χ^2=3.5 for 9:3:3:1 accepted at 95% confidence.
†Data represent the mean and standard error for length of the primary root at 10 days postgermination in several seedlings of each genotype.

We also followed a genetic approach to this question, taking advantage of available mutants of *Arabidopsis* that are defective in auxin response. Two *Arabidopsis* genes involved in auxin response (*AXR1, AXR2*) have been identified by selection for mutations conferring resistance to exogenous 2,4D (Estelle and Somerville, 1987; Lincoln et al., 1990; Timpte et al., 1994). Sequence analysis of the *AXR1* gene shows that it encodes a protein related to the ubiquitin-activating enzyme E1 (Leyser et al., 1993). The *axr1* mutations were identified by auxin-resistant growth of the root system, but the mutations also generate curled, serrated rosette leaves with short petioles, and a highly branched inflorescence indicating that the gene has a function in the aerial portion of the plant. We constructed *axr1-3,lop1* and *axr1-12,lop1* double mutants to test the idea that *lop1* is an auxin overproducer. We reasoned that if the *lop1* phenotype resulted from overproduction of auxin, then the response defect of *axr1* would abolish this phenotype in double mutants. Double heterozygotes were constructed and their F_2 progeny segregated each of the single mutants and a rare class representing the *axr1,lop1* double mutants, as shown in Table 3. The rosette leaves of double mutants were curled and serrated (*axr1*-like) and twisted (*lop1*-like), showing evidence of both mutant phenotypes. We also observed inhibition of root growth characteristic of *lop1* in the double mutants, as shown in Table 3. These results show that *axr1* does not abolish the *lop1* phenotype, and together with the GC-SIM-MS data indicate that *lop1* is not an overproducer of IAA.

Auxin response

Inhibition of primary root growth by exogenous auxin is a well-characterized trait employed in identification of *Arabidopsis* mutants defective in auxin response (Lincoln et al., 1990). Our dose response curves with wild-type *Arabidopsis* indicated that root growth in the interval between 6 and 12 days post-germination was reduced 50% by 3×10^{-8} M 2,4D. To determine whether the *lop1* mutation affected auxin response, growth of primary roots was compared in mutant and wild-type seedlings in the presence and absence of 3×10^{-8} M 2,4D, as shown in Fig. 6. Wild-type control roots grew to an average length of 6.3 cm by 12 days, as opposed to 2.9 cm in the presence of 2,4D. Mutant roots grew slower than wild-type on the control medium, reaching an average length of only 1.7 cm, but in the presence of 2,4D, root length was further reduced by 50% to 0.7 cm. Further, it was observed that mutant and wild-type seedlings similarly displayed cessation of root growth at 6×10^{-8} M 2,4D (data not shown). Thus, auxin perception does not appear to be altered in the *lop1* mutant.

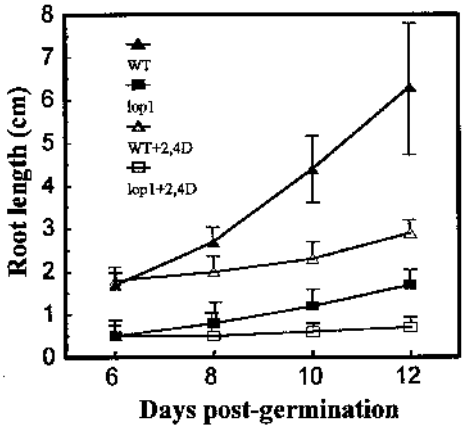

Fig. 6. Root growth in wild-type and the *lop1* mutant in the presence and absence of exogenous 2,4D. Data represent the average length of the primary root in five seedlings/genotype.

Auxin transport

Auxin is produced primarily in young leaf primordia at the shoot apex and transported in a basipetal direction (downward) in the stem. Excised stem segments retain this pattern of basipetal transport, translocating labeled IAA preferentially from the apical end to the basal end of the segment (Okada et al., 1991). Non-specific acropetal transport from the basal to the apical end provides the appropriate control. Data in Fig. 7 show that basipetal IAA transport in the mutant is only slightly above non-specific acropetal transport whereas, wild-type controls show about a ten-fold increase in basipetal vs. acropetal transport. These results indicate that the *lop1* mutant is defective in basipetal transport of IAA.

DISCUSSION

The ability to impose precise controls over the extent and the polarity of cell expansion is one of the most fundamental elements of pattern formation in higher plants. It is well known that auxin is a key player in this aspect of cellular growth, and accordingly this plant hormone affects a very broad range of developmental pathways. Even its effect on differentiation of vascular tissue is thought to be associated with the induction of polarized cell elongation and subsequent formation of specialized channels for auxin transport (Sachs, 1991). The principal challenge with the auxin pathway has been to determine the molecular basis for its specificity, and this picture is now emerging from the identification of genes and proteins involved in auxin synthesis (Boerjan et al., 1995), transport (Lomax et al., 1995; Okada et al., 1991) and perception (Leyser et al., 1993). In particular, there has been progress toward understanding mechanisms for auxin transport. Directional flow appears to be established by localization of IAA efflux carriers at the basipetal end of transporting cells (Lomax et al., 1995), and there is some evidence that the process is regulated by flavonoids (Rubery and Jacobs, 1990) and other regulatory proteins (Lomax et al., 1995). There are as yet, however, no molecular probes or loss-of-function mutations identified for these components of the transport pathway.

Our histological and biochemical analysis of *lop1* mutant

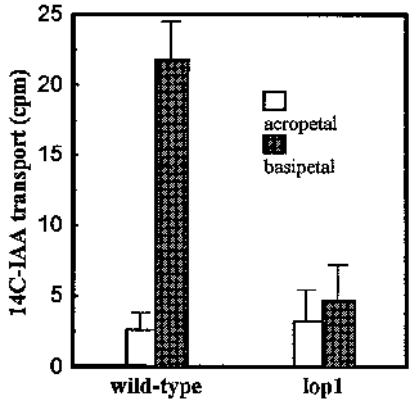

Fig. 7. Transport of [^{14}C]IAA in stems of wild-type and the *lop1* mutant of *Arabidopsis.* Transport assays were conducted in four separate experiments on stem sections (length=2.5 cm) excised from several individuals of each genotype. Data represent the average counts per minute of [^{14}C]IAA determined by liquid scintillation. Acropetal movement of IAA represents non-specific transport from the basal to the apical end of the stem segment. Basipetal movement of IAA represents transport from the apical to the basal end of the stem segment.

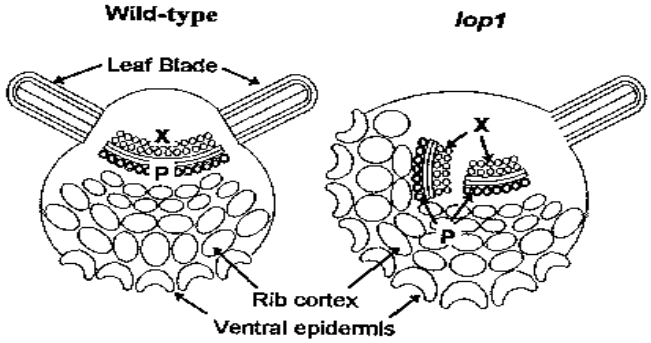

Fig. 8. Transverse anatomy of the leaf midrib in wild-type and the *lop1* mutant of *Arabidopsis.* The drawing shows representative anatomical aberrations observed in *lop1* mutant leaves. The wild-type midvein displays bilateral symmetry, with xylem cells (X) facing the dorsal surface and phloem cells (P) facing the ventral surface. Mutant leaves show midvein bifurcation and vein rotation. One-sided loss of blade formation is associated with precocious radial expansion of cortical cells on the lateral flank of the primordium.

plants provide several lines of evidence that this mutation generates a primary defect in the auxin transport pathway. Foremost is the transport assay itself showing that mutants stems are defective in basipetal movement of labeled IAA (Fig. 7), whereas auxin perception (Fig. 6) and overall levels of free IAA appear normal. Further, the disoriented growth of the midvein in *lop1* mutants (Figs 3D, 4C) and particularly the midvein bifurcation (Fig. 3G) are mutant phenotypes that are consistent with an early disruption in patterns of auxin transport in young primordia. It remains unclear how a transport defect would generate the vein rotation observed in mutant petioles (Fig. 4F,H). Transport patterns may have some role in determination of dorsal/ventral orientation of developing veins, but alternatively it is possible that this phenotype is a secondary consequence of abnormal growth in the surrounding cortical tissue.

The abnormal patterns of cell expansion observed in *lop1* mutants also seem consistent with a primary defect in auxin transport. In dicot stems, the elongated parenchyma cells associated with veins are the main conduit for auxin transport (Jacobs and Gilbert, 1983), and lateral movement of IAA from these cells is known to affect cell expansion in the surrounding cortex (Sanchez-Bravo et al., 1991). We observed formation of oversized midribs in mutant leaves that results primarily from precocious radial expansion of the cortical cells (Table 2). Histological analysis revealed that abnormal expansion patterns are detectable at early stages in leaf development (Fig. 4J), particularly along the lateral flanks of the primordium and often in association with a loss of blade formation (Fig. 4K). Abnormal auxin transport by vascular-associated parenchyma cells may lead to auxin accumulation and excess lateral movement into the cortex where it generates precocious cell expansion. It is also possible that vein rotation is partially responsible for abnormal patterns of cortical development. Our analysis of wild-type midribs shows that cortical expansion always begins with cells adjacent to the phloem pole on the ventral side of the midvein (Fig. 2G-I), suggesting that phloem-associated parenchyma may be more active in IAA transport. Vein rotation shifts the orientation phloem poles out of the normal dorsal/ventral axis in mutant midribs, as illustrated in Fig. 8. This could result in abnormal cell expansion patterns in the cortex, having the net effect of increasing the circumferential extent of rib formation at the occasional expense of blade development.

Finally, the abnormal development of lateral roots (Figs 3J and 5D), and disorganized patterns of epidermal cell expansion in the root elongation zone (Fig. 5B) of the mutant are also consistent with a disruption in the auxin pathway. Epidermal cells of the elongation zone are well known target sites for auxin-mediated growth regulation, and further it is known that there are two distinct auxin transport streams in plant roots, one moving acropetally through the stele, and another moving basipetally in the epidermis (Lomax et al., 1995; Jones, 1990; Tsurumi and Ohwaki, 1978). Application of exogenous IAA has shown that elongation growth of roots is controlled primarily by basipetal transport through the epidermis (Davies et al., 1976). Defective basipetal transport in epidermal cells thus represents a reasonable explanation for the abnormal patterns of cell expansion and general disorganization of the *lop1* root elongation zone. A disruption in epidermal transport might lead to localized accumulation of IAA, and associated abnormalities in basic patterns of cell expansion. This epidermal disruption is correlated with a twisted morphology in the roots, and may be the cause of this abnormal growth pattern. But just how adjacent epidermal cells manage to elongate collectively in the wrong direction to generate a repeating dextral or sinistral spiral remains an unanswered question.

Although these shoot and root phenotypes in the mutant point to a defect in auxin transport, it is still uncertain as to whether the *LOP1* gene product actually plays a direct role in this process. For example it is possible that the *lop1* mutation disrupts some fundamental aspect of cellular organization which then produces the transport defect as a secondary consequence (Gersani et al., 1986). Nonetheless it appears that *lop1* has a rather specific effect on transport, as opposed to mutations at the *PIN-FORMED* locus (chromosome 1) in *Arabidopsis*, which produce a disruption in transport (14% of wild-type) and a deficiency in levels of free IAA (8% of wild-type; Okada et al., 1991). The *pin1* mutant plants generate abnormal

flowers, or a spike inflorescence lacking floral buds altogether. Mutants also have fused cotyledons, and split midveins in the leaves, indicating a role for this gene in early stages of embryogenesis and in subsequent vegetative development. The *lop1* mutation produces split midveins like *pin1*, but otherwise the phenotypes are quite distinct. In particular, *lop1* has no effect on cotyledon morphology, and allows a normal pattern of floral initiation. This may be related to the different levels of free IAA in these mutants. Free IAA levels are normal in *lop1*, but drastically reduced in *pin1*, which may account for the broad spectrum of abnormalities observed there. The IAA deficiency in *pin1* was considered a secondary consequence of the transport lesion (Okada et al., 1991), perhaps due to feedback regulation linking IAA biosynthesis and transport. Our results with *lop1* show normal biosynthesis in spite of a major transport defect, which argues against feedback regulation.

Genetic approaches are certain to play an indispensable role in dissecting the myriad aspects of development connected to auxin biology. Mutations knocking out one function at a time may provide the only straightforward means of identifying functionally distinct branches of this complicated pathway. The *lop1* mutant, for example, has abnormal shoots and roots but its cotyledon phenotype is normal. Since polar transport is an essential feature of normal embryogenesis (Cooke et al., 1993), this suggests that *LOP1* functions primarily in the post-embryonic phase of development. In contrast, the *pin1* mutation appears to have its most prominent effect in the embryo and in the emerging inflorescence. Molecular analysis of *LOP1* and *PIN1* gene products, together with continued genetic dissection should lead eventually to a better understanding of the auxin pathway and its far reaching effects in plant development.

We thank Dr Jennifer Normanly (Dept. of Biochemistry and Molecular Biology, University of Massachusetts) for generous advice and assistance with the GC-SIM-MS auxin assay, Dr Stephen Dellaporta (Dept. of Biology, Yale University) for his participation in the T-DNA screen, and Dr Timothy Nelson (Dept. of Biology, Yale University) for invaluable counsel. We gratefully acknowledge the technical assistance of Regan Huntley and Ruben Ruiz. This work was partially supported by a USDA/NRI grant to N. A. M.

REFERENCES

Abeles, F. B., Morgan, P. W. and Saltveit, Jr., M. E. (1992). *Ethylene in Plant Biology*, pp 147-156, San Diego, CA: Academic Press.

Bell, C. J. and Ecker, J. (1994). Assignment of 30 microsatellite loci to the linkage map of *Arabidopsis*. *Genomics* **19**, 137-144.

Boerjan, W., Cervera, M. T., Delarue, M. Beeckmen, T., Dewitte, W., Bellini, C., Caboche, M., Van Onckelen, H., Van Montagu, M. and Inze, D. (1995). *superroot*, a recessive mutation in *Arabidopsis*, confers auxin overproduction. *The Plant Cell* **7**, 1405-1419.

Chen, K. H., Miller, A. N., Patterson, G. W. and Cohen, J. D. (1988). A rapid and simple procedure for purification of indole-3-acetic acid prior to GC-SIM-MS analysis. *Pl. Physiol.* **86**, 822-825.

Cooke, T. J., Racusen, R. H. and Cohen, J. D. (1993). The role of auxin in plant embryogenesis. *The Plant Cell* **5**, 1494-1495.

Davies, P. J., Doro, J. A. and Tarbox, A. W. (1976). The movement and physiological effect of indole-acetic acid following point applications to root tips of *Zea mays*. *Physiol. Plant.* **36**, 333-337.

Dellaporta, S. (1994). Plant DNA miniprep and microprep: versions 2. 1-2. 3. In *The Maize Handbook.* (eds M. Freeling and V. Walbot). Springer-Verlag, New York, NY. pp. 522-525.

Estelle M. A. and Somerville, C. (1987). Auxin-resistant mutants of *Arabidopsis thaliana* with an altered morphology. *Mol. Gen. Genet.* **206**, 200-206.

Fabri, C. O. and Schaffner, A. R. (1994). An *Arabidopsis thaliana* RFLP mapping set to localize mutations to chromosomal regions. *The Plant J.* **4**, 149-156.

Gersani, M., Leshem, B. and Sachs, T. (1986). Impaired polarity in abnormal plant development. *J. Pl. Physiol.* **123**, 91-95.

Guzman, P. and Ecker, J. R. (1990). Exploiting the triple response of *Arabidopsis* to identify ethylene-related mutants. *The Plant Cell* **2**, 513-523.

Hauge, B. M., Hanley, S. M., Cartinhour, S., Cherry, J. M., Goodman, H. W., Koorneef, M., Stam, P., Chang, C., Kempin, S. Medrano, L. and Meyerowitz, E. M. (1993). An integrated genetic/RFLP map of the *Arabidopsis thaliana* genome. *The Plant J.* **3**, 745-754.

Jacobs, M. and Gilbert, S. (1983). Basal localization of the presumptive auxin transport carrier in pea stem cells. *Science* **220**, 1297-1300.

Jacobs, W. P., Morrow, I. (1957). A quantitative study of xylem development in the vegetative shoot apex of *Coleus*. Am. J. Bot. **44**, 823-842.

Jones, A. M. (1990). Location of transported auxin in etiolated maize shoots using 5-azidoindole-3-acetic acid. *Pl. Physiol.* **93**,1154-1161.

Klee, H. J., Horsch, R. B., Hinchee, M. A., Hein, M. B. and Hoffmann, N. L. (1987). The effects of overproduction of two *Agrobacterium tumefaciens* T-DNA auxin biosynthetic gene products in transgenic petunia plants. *Genes Dev.* **1**, 86-96.

Kosambi, D. D. (1944). The estimation of map distances from recombination values. *Ann. Eugen.* **12**, 172-175.

LaMotte, C. E. and Jacobs, W. P. (1963). A role of auxin in phloem regeneration in *Coleus* internodes. *Dev. Biol.* **8**, 80-98.

Lander, E. S, Green, P., Abrahamson, J., Barlow, A., Daly, M. J., Lincoln, S. E. and Newburg, L. (1987). MAPMAKER: An interactive computer package for constructing primary genetic linkage maps of experimental and natural populations. *Genomics* **1**, 174-181.

Leyser, H. M. O., Lincoln, C. A., Timpte, C., Lammer, D., Turner, J. and Estelle, M. (1993). *Arabidopsis* auxin-resistance gene AXR1 encodes a protein related to ubiquitin-activating enzyme E1. *Nature* **364**, 161-164.

Lincoln, C., Britton, J. H., Estelle, M. (1990). Growth and development of the *axr1* mutants of *Arabidopsis*. *Plant Cell* **2**, 1071-1080.

Lomax, T. L., Muday, G. K. and Rubery P. H. (1995). Auxin transport, In PJ Davies, ed, Plant Hormones: Physiology, Biochemistry and Molecular Biology. Kluwer Academic, pp 509-530.

McHale, N. A. (1993). LAM1 and FAT genes control development of the leaf blade in *Nicotiana sylvestris. The Plant Cell* **5**, 1029-1038.

Murashige, T. and Skoog, F. (1962). A revised medium for rapid growth and bioassays with tobacco tissue cultures. *Physiol. Plant.* **15**, 473-497.

Normanly, J., Slovin, J. P. and Cohen, J. D. (1995). Rethinking auxin biosynthesis and metabolism. *Plant Physiol.* **107**, 323-329.

Okada, K., Ueda, J., Komaki, M. K., Bel, C. J. and Shimura, Y. (1991). Requirement of the auxin polar transport system in early stages of *Arabidopsis* floral bud formation. *Plant Cell* **3**, 677-684.

Romano, C. P., Hein, M. B. and Klee, H. J. (1991). Inactivation of auxin in tobacco transformed with the indoleacetic acid-lysine synthetase gene of *Pseudomonas savastanoi*. *Genes Dev.* **5**, 438-446.

Rubery, P. H., Jacobs, M. (1990). Auxin transport and its regulation by flavonoids. In: *Plant Growth Substances 1988,* (ed. Pharis, R. P., Rood, S. B.), pp. 428-440. Berlin: Springer Verlag.

Sachs, T. (1991). Cell polarity and tissue patterning in plants. *Development* **Supplement 1**, 83-93.

Sambrook, J. E., Fritsch, E. F. and Maniatis, T. (1989). *Molecular Cloning: A Laboratory Manual*. Cold Spring Harbor, N. Y: Cold Spring Harbor Laboratory.

Sanchez-Bravo, J., Ortuno, A., Botia, J. M., Acosta, M. and Sabater, F. 1991. Lateral diffusion of polarly transported indoleacetic acid and its role in the growth of *Lupinus albus* L. hypocotyls. *Planta* **185**, 391-396

Shininger, T. L. (1979). The control of vascular development. *Annu. Rev. Plant Physiol.* **30**, 313-337.

Timpte, C., Wilson, A. K. and Estelle, M. (1994). The *axr2-1* mutation of *Arabidopsis thaliana* is a gain-of-function mutation that disrupts an early step in auxin response. *Genetics* **138**, 1239-1249.

Tsurumi, S. and Ohwaki, Y. (1978). Transport of 14C-labeled indoleacetic acid in *Vicia* root segments. *Plant Cell Physiol.* **19,** 1195-1206.

Wangermann, E. (1967). The effect of the leaf on differentiation of primary xylem in the internode of *Coleus*. *New Phytol.* **66**, 747-754.

Wetmore, R. H. and Rier, J. P. (1963). Experimental induction of vascular tissures in callus of angiosperms. *Am. J. Bot.* **50**, 418-430.

Young, G. S. (1954). The effects of leaf primordia on differentiation in the stem. *New Phytol.* **53**, 445-460.

(Accepted 1 March 1996)